

Human Bone Marrow Mesenchymal Stem Cell-derived Extracellular Vesicles Restore Th17/Treg Homeostasis in Periodontitis via miR-1246


Yuxing Xia
Tianfan Cheng
Chengfei Zhang
Min Zhou
Zhekai Hu
Feiwu Kang (✉ kfw@tongji.edu.cn)
Chongshan Liao (✉ liao-chongshan@tongji.edu.cn)

Research Article

Keywords: Periodontal disease, Stem cell, microRNA, Angiotensin-converting enzyme 2 (ACE2), Yes-associated protein 1 (YAP1)

Posted Date: March 30th, 2023

DOI: <https://doi.org/10.21203/rs.3.rs-1961434/v2>

License:  This work is licensed under a Creative Commons Attribution 4.0 International License.
[Read Full License](#)

Abstract

T-cell-mediated immunity is crucial in the immunopathology of periodontitis. The restoration of the equilibrium between the T helper cell 17 (Th17) and regulatory T cell (Treg) subsets by extracellular vesicles (EVs) obtained from human bone marrow stem cells (hBMSCs) promotes new bone formation and suppresses inflammation. Uncovering the functions of hBMSC-derived EVs in the immune microenvironment of periodontal tissue and their underlying regulatory mechanisms may shed new light on the development of a potential cell-free immunotherapy for periodontal regeneration. Here we report that the Th17/Treg ratio was elevated in peripheral blood from periodontitis patients. Furthermore, we found that hBMSC-derived EVs could reduce the Th17/Treg ratio in CD4⁺ T cells from periodontitis patients *in vitro* and ameliorated experimental periodontitis in mice. Additionally, miRNA sequencing was used to investigate the differentially expressed miRNAs and target genes in EVs from hBMSCs stimulated with *P. gingivalis* LPS. Our findings indicate that EV-miR-1246 is highly effective at down-regulating the ratio of Th17/Treg *in vitro*. Mechanistically, EV-miR-1246 suppressed angiotensin-converting enzyme 2 (ACE2) expression and increased the p-Yes-associated protein (YAP)1/YAP1 ratio in CD4⁺ T cells. Our results indicate that hBMSC-derived EVs improve periodontitis by miR-1246, consequently downregulating Th17/Treg ratio, and represent a promising therapeutic target for precision treatment in periodontitis.

Background

Periodontitis, a prevalent inflammatory disease of the periodontium, is a major contributor to alveolar bone resorption and tooth loss in adult population. This disease is associated with significant global burden and has profound socioeconomic impacts worldwide [1]. The host-microbe relationship imbalance in the oral cavity dysregulates the immuno-inflammatory response, initiating periodontal destruction [2,3]. The recruitment of a surplus of neutrophils and secretion of proinflammatory cytokines interleukin (IL)-17 and orphan receptor gamma transcription (ROR γ t) by T helper 17 (Th17) lead to the osteoclast-mediated destruction of periodontal tissue and alveolar bone [4,5]. Our previous studies revealed that IL-17 promoted bone resorption through osteocyte-specific signaling pathways and regulated the osteogenesis of mesenchymal stem cells (MSCs) [6,7,8]. In contrast, regulatory T (Treg) cells, which express forkhead box P3 (FOXP3) and interleukin (IL)-10 are involved in immunosuppression and tissue repair, which are critical for the maintenance of periodontal health [9]. An elevated Th17/Treg ratio in peripheral blood is reportedly associated with periodontal inflammation and alveolar bone destruction [10]. Notably, an imbalance in the Th17/Treg ratio contributes to the development of periodontitis [11].

MSC-based tissue engineering therapy has considerable potential for periodontal regeneration in clinical practice [12,13]. However, the effectiveness of MSCs in periodontal treatment is hindered by challenges such as low tissue retention, low survival rate, and difficulty controlling cell fate [14]. It is worth noting that MSCs exhibit significant immunomodulatory effects via paracrine communication, particularly through the secretion of EVs [15,16]. These EVs, which are abundant in miRNAs and proteins and derived from

human bone marrow MSCs (hBMSCs), have been shown to effectively suppress macrophage inflammatory responses, and promote periodontal regeneration [17,13].

In various aspects of eukaryotic life, miRNAs, which are small non-coding RNAs, modulate gene expression, primarily via RNA-silencing mechanisms [18]. The levels of various miRNAs (e.g., miR-17, miR-19, miR-155, and miR-301) are significantly increased in periodontitis patients compared with healthy controls. Such increases are closely associated with the progression of periodontal disease [19,20]. In addition, miRNAs also have regulatory effects on T-cell differentiation and macrophage polarization [21]. In an experimental periodontitis mice model, EV-miRNAs derived from dental pulp stem cells can restore Th17/Treg homeostasis [22]. However, the therapeutic applications of MSC-derived EVs and EV-miRNAs remain limited in terms of restoring Th17/Treg homeostasis in periodontitis.

The target of MSC-derived EV-miRNAs on cluster of differentiation (CD)4⁺ T cells during periodontitis remains unclear, and subsequent pathways have not been elucidated. Recent evidence has highlighted that angiotensin-converting enzyme 2 (ACE2), a key T-cell receptor involved in infectious diseases [23], can be stimulated by miR-146a and miR-155 in the periodontal inflammatory microenvironment [24]. Moreover, Yes-associated protein 1 (YAP1), an important protein in the Hippo signaling pathway, can restrict CD4⁺ T-cell activation and proliferation [25,26]. These studies suggest that MSC-derived EV-miRNAs may regulate the Th17/Treg ratio among CD4⁺ T cells via ACE2 and YAP1 signalings in periodontitis. Therefore, this study aims to investigate whether hBMSC-derived EVs and their key miRNAs affect the Th17/Treg ratio among CD4⁺ T cells in periodontitis and the downstream pathways.

Materials And Methods

Participant Recruitment

This study protocol was approved by the Ethics Committee of the Stomatological Hospital of Tongji University (Approval No. 2020-R-011), and the study adhered to the Declaration of Helsinki. Each participant provided written informed consent to take part in the study, and they legally authorized their next of kin to oversee the use of any biological sample. Periodontitis was selected with probe depth ≥ 5 mm in at least four teeth with each ≥ 1 site, clinical attachment level ≥ 5 mm on the same site, and observed bleeding upon probing. The periodontal disease diagnosis followed the World Workshop 2017 criteria [27]. All participants met the following inclusion criteria: presence of periodontitis, age 18–40 years, and no systemic disease. The exclusion criteria were consumption of antibiotics or anti-inflammatory medications within the preceding 3 months, previous periodontal treatment, any systemic diseases that may affect periodontal conditions (e.g., immunodeficiency or pregnancy), and a history of smoking (past or present). Detailed participant data are shown in Appendix Table 1.

Analysis of peripheral blood from human participants

RNA and serum were extracted from the fasting peripheral blood of eight healthy volunteers and eight periodontitis patients (age 18–40 years). Total RNA was extracted from peripheral blood and reverse transcribed to single-stranded cDNA with a PrimeScript™ RT Reagent Kit (Takara, Nojihigashi, Japan). Quantitative reverse transcription PCR (qRT-PCR) was conducted using the CFX96™ Real-Time PCR Detection System (Bio-Rad, Hercules, CA, USA). The sequences of primers for human *RORC* and *FOXP3* (Sangon Biotech, Shanghai, China) are shown in Appendix Table 2. Serum levels of IL-17A and FOXP3 were measured using corresponding enzyme-linked immunosorbent assay (ELISA) kits (Abcam, Cambridge, UK), in accordance with the manufacturer's protocol.

hBMSC extraction and identification

The cancellous bone marrow was extracted from discarded maxilla bone tissue of 5 orthognathic patients (3 females and 2 males, 18-25 years old) with good oral health in the Stomatological Hospital of Tongji University. The bone marrow was washed with PBS once and then resuspended with minimum essential medium Alpha (α -MEM, Hyclone, Utah, USA) containing 10% fetal bovine serum (Gibco, Waltham, MA, USA) and 1% penicillin/streptomycin (Hyclone, Utah, USA). When the confluence reached about 80%, the cells were digested by trypsin/EDTA. The cells at passage 3 were assessed by flow cytometry analysis with the surface markers CD90, CD73, CD44, and CD105, using the Human MSC Analysis Kit (B.D. Biosciences, San Jose, CA).

hBMSC-derived EVs extraction and identification

When hBMSCs grew to 80% confluence, the medium was replaced with serum-free α -MEM. After 48 hours, the medium was concentrated to 1/10 of the original volume in an Amicon® Ultra 15 mL Centrifugal Filters (Membrane NMWL 100 KDa, Millipore, Bedford, MA) at 800 g for 5 min. And then, the concentrates were transferred to a sterile container, mixed with an appropriate amount of ExoQuick precipitation solution (Invitrogen, Carlsbad, USA), and incubated at 4 °C for 16 hours. The EV pellet was collected by centrifugation at 10,000 g, 4 °C for 2 hours, and resuspended with 200 μ l PBS.

EVs stained with antibodies against CD63 and CD81 were examined by flow cytometry using a BD LSRFortessa™ Cell Analyzer (B.D. Biosciences), and the data were analyzed using FlowJo v7.6. For the Transmission electron microscope (TEM) analysis, samples were dried and examined under an electron microscope (FEI, Tecnai G2 F20 S-TWIN, USA). For the nanoparticle tracking analysis (NTA), the pellets collected from programmed centrifugation were resuspended in PBS. Then the size of the vesicles was detected using a nanoparticle tracing assay (NanoSight, Particle Metrix, Meerbusch, German).

Isolation of naïve CD4⁺ T cells from periodontitis patients (PD-CD4⁺ T cells)

Peripheral blood mononuclear cells (PBMCs) were isolated from the blood of five periodontitis patients' blood using Ficoll-Paque gradient centrifugation (GE Healthcare, Madison, WI, USA). PD-CD4⁺ T cells were prepared from pooled PBMCs via positive selection by depletion of non-T lymphocytes using a human naïve CD4⁺ T cell isolation kit (Miltenyi Biotechnologies, Teterow, Germany), in accordance with the manufacturer's instructions.

Analysis of PD-CD4⁺ T-cell differentiation

For EVs group, PD-CD4⁺ T cells were incubated for 24 hours with hBMSC-derived EVs (10 µg/mL) from healthy volunteers. Flow cytometry was used to identify differentiated Th17 and Treg cells. After incubation with phycoerythrin-labeled anti-CD4, allophycocyanin-labeled anti-IL17A, and fluorescein isothiocyanate-labeled anti-FOXP3 antibodies in FIX & PERM cell permeabilization reagents (Invitrogen, California, USA), cells were examined using a BD LSRFortessa™ Cell Analyzer (BD Biosciences, New Jersey, USA); the resulting data were analyzed using FlowJo v7.6. Additionally, mRNA expression levels of *RORC*, *FOXP3*, *IL10*, and *IL17A* in PD-CD4⁺ T cells were analyzed by qRT-PCR. The primer sequences are shown in Appendix Table 2.

Internalization of EVs by PD-CD4⁺ T Cells

EVs were labelled with PKH67 Green Fluorescent Cell Linker Kit (Umibio, Shanghai, China). The stained EVs were mixed into PD-CD4⁺ T cells resuspended in RPMI 1640 medium and cultured for 12 hours. The nucleus was stained with DAPI (Sigma, USA). Observation and photographing were performed under a microscope (NIKON ECLIPSE 80i, Nikon Corporation).

Animals

Eighteen male C57BL/6J mice (7 weeks of age, weighing 22–24 g; Leagene Biotech, Shanghai, China) were used in this study. All animal procedures were approved by the Institutional Animal Care and Use Committee of the Stomatological Hospital of Tongji University (Approval No. 2020-DW-026). A prospective randomized controlled animal model design was adopted, in accordance with the Animal Research: Reporting *In Vivo* Experiments (ARRIVE) guidelines. Mice were anesthetized by intraperitoneal injection of ketamine (200mg/kg) .

Ligature-induced periodontitis model and EVs treatment

Mice were randomly allocated to the following groups: control, periodontitis (perio; with ligation); hydrogel (hydrogel application after ligation); hydrogel + EVs (hydrogel + EV application after ligation). Silk sutures (6–0) were placed on the upper second molars of mice without causing damage to periodontal tissues [28]. On day 7, silk threads were removed after observance of clinical signs of gingival inflammation (swelling, redness, and loss of gingival adhesion to the tooth). Mice in the control (n = 6) and perio groups (n = 6) were sacrificed on day 7 for qRT-PCR and micro-computed tomography (CT) analysis.

Beginning on day 8, the remaining mice with ligature-induced periodontitis received local treatment comprising hydrogel (n = 3) or hydrogel + EVs (n = 3). To prepare EV-loaded hydrogel, 40 mg of polyether F127 thermosensitive hydrogel (EngineeringForLife, Suzhou, China) were added to 200 μ L of EV-phosphate-buffered saline (PBS; 1 μ g EVs/1 μ L PBS) suspension. Every other day, 10 μ L of hydrogel with or without EVs were injected into periodontal pockets using a 26-gauge syringe (Hamilton Company, Reno, NV, USA). Mice in the hydrogel and hydrogel + EVs groups were sacrificed on day 14.

Histomorphological analysis and immunofluorescence

The maxillae were fixed, decalcified, and stained with hematoxylin & eosin (H&E, KeyGen, Nanjing, China). The distance between the cemento-enamel junction and alveolar bone crest (CEJ-ABC) was measured to evaluate the bone loss. For immunofluorescence, the sections were then incubated with either anti-ROR γ antibody or anti-FOXP3 antibody (Appendix Table 3), then incubated with secondary antibody Alexa Fluor-488 (green) or Alexa Fluor-594 (red) after PBS washes. Negative control sections were set by omitting the primary antibodies. The sections were mounted with DAPI and examined under a microscope (NIKON ECLIPSE 80i, Nikon Corporation).

Micro-computerized tomography (micro-CT)

micro-CT was used to quantify bone remodeling using the Scanco Medical μ CT50 system and related analysis software. A region of interest (ROI) that contained the areas of maxillae was selected. The key parameters were set as follows: 70 kV, 110 mA, and 10- μ m increments. For quantifying trabecular bone volume/total volume (BV/TV), a total of 300 μ m (30 layers) of the alveolar bone between the first and second molars were analyzed.

miRNA sequencing (miRNA-seq)

hBMSCs were treated with 1 μ g/mL of *Porphyromonas gingivalis* lipopolysaccharide (*P. g.* LPS, Sigma-Aldrich, St Louis, USA) for 24 hours, and the corresponding EVs were isolated. Small RNAs were isolated

from the EVs for miRNA-seq. The miRNA-seq libraries were prepared and sequenced using an Illumina HiSeq (Illumina, San Diego, USA) at Wayen Biotechnologies, Inc., (Shanghai, China). Feature counts were used to determine read counts, and DESeq2 was used to analyze differential expression (genes with a corrected p-value < 0.05 and an absolute \log_2 fold change > 2).

Transfection of miR-1246

miR-1246 mimic, inhibitor, nc on and nc off (Ribobio, Guangzhou, China) were transfected into healthy hBMSCs for 48 hours using Lipofectamine 2000 (Invitrogen, Carlsbad, CA) according to the manufacturer's protocols. The efficiency of transfection was checked by qRT-PCR. The primers used in the process are shown in Appendix Table. 2. Human *miR-1246* was normalized to *U6 (RNU6-1)*.

Western blot

The polyvinylidene fluoride membrane onto which separated proteins was transferred was immunoblotted with primary antibodies against human YAP1 (Abcam), human P-YAP1 (S127) (Abcam), human ACE2 (Abcam), mouse ROR γ (Affinity), mouse FOXP3 (Affinity), and human / mouse β -actin (Affinity). The antibody concentration was shown in Appendix Table. 3. The protein bands were visualized with enhanced chemiluminescence and imaged using an Amersham™ Imager 680 (G.E. Healthcare Bio-Sciences, Uppsala, Sweden).

Target gene prediction and dual luciferase reporter assay

miR-1246 target genes were selected using miRDB, miRWalk, and TargetScan. The ACE2 gene, which was associated with miR-1246, was selected for further investigation. miR-1246-binding sites on the 3'-untranslated region (UTR) of ACE2 were identified via TargetScan online bioinformatics software. Dual luciferase activity was analyzed using a dual luciferase assay kit (Promega, Madison, WI, USA) in accordance with the manufacturer's instructions. Briefly, ACE2 recombinant plasmids (ACE2-WT and ACE2-Mut) and mimic N.C. or miR-1246 were transfected into 293T cells.

Data analysis

Results represent independent experiments ($n \geq 3$); Data were presented as mean \pm standard deviation. A 2-tailed Student's *t*-test was used for comparison between 2 groups, and one-way analysis of variance test was used for multiple comparisons. $P < 0.05$ was considered statistical significance. All statistical analyses were performed using GraphPad Prism software (version 9.0).

Results

Identification of hBMSCs and EVs

hBMSCs with fibroblast-like were isolated from the discarded maxillae of periodontally healthy volunteers during orthognathic surgery (Fig. 1A). The osteogenic and adipogenic characteristics of the cells were confirmed by means of alizarin red and oil red O staining (Fig. 1A, C). The stemness properties of hBMSCs were assessed by flow cytometry focused on surface markers (CD90, CD44, CD105 and CD73) (Fig. 1D). hBMSC-derived EVs exhibited round or tea receptacle microvesicle structures with diameters of 100–400 nm (Fig. 1E, F) and were found to express the surface markers CD63 and CD81 (Fig. 1G).

Peripheral levels of Th17- and Treg-related biomarkers in periodontitis patients

The presence of biomarkers for Th17 and Treg cells was evaluated in peripheral blood from periodontitis patients and healthy volunteers. mRNA expression analysis revealed that the level of *RORC* was significantly upregulated and the level of *FOXP3* was downregulated in periodontitis patients, compared with healthy volunteers (Fig. 2A). Consistent with these findings, ELISA showed that the serum level of IL-17A was significantly greater in periodontitis patients than in healthy controls; conversely, the serum level of FOXP3 was significantly lower in periodontitis patients (Fig. 2B) ($P < 0.001$). These results implied that periodontitis disrupts immune homeostasis by enhancing Th17 function and impairing Treg function.

Periodontally healthy hBMSC-derived EVs restored the Th17/Treg ratio in PD-CD4⁺ T cells

PD-CD4⁺ T cells were isolated from PBMCs of periodontitis patients (Fig. 2C, Appendix Fig. 1). PKH67-labeled EVs were internalized in PD-CD4⁺ T cells after co-incubation for 12 hours. (Fig. 2D). Flow cytometry assays revealed that EVs reduced the proportion of Th17 cells by 60% ($P < 0.01$) while increasing the proportion of Treg cells by 10% ($P < 0.05$); these changes led to significant downregulation of the Th17/Treg ratio ($P < 0.05$) (Fig. 2E, F). Consistently, stimulation with hBMSC-derived EVs led to > 50% reduction in the mRNA expression levels of *RORC* and *IL17A* in PD-CD4⁺ T cells ($P < 0.05$). In contrast, the mRNA expression levels of *IL10* and *FOXP3* were significantly increased ($P < 0.01$) (Fig. 2G). The data suggested that hBMSC-derived EVs from healthy volunteers possess the potential to mitigate the imbalance in Th17/Treg differentiation from PD-CD4⁺ T cells *in vitro*.

Healthy hBMSC-derived EVs promoted bone regeneration in vivo

Because hBMSC-derived EVs showed beneficial immune modulation effects *in vitro*, we further examined whether hBMSC-derived EVs could promote periodontal recovery *in vivo*. As shown in the schematic

diagram of animal treatment (Fig. 3A and B), the mRNA expression levels of *Rorc* and *Il17a* were significantly upregulated in ligature-induced periodontitis (LIP) mice, compared with healthy mice; in contrast, the *Foxp3* and *Il10* mRNA expression levels were significantly downregulated in LIP mice (Fig. 3C). Hematoxylin and eosin staining indicated that the bone resorption level (cemento-enamel junction to alveolar bone crest) was significantly lower in the group that received EV-loaded hydrogel than in the group that received hydrogel alone ($P < 0.01$, Fig. 3D). Furthermore, micro-CT analysis showed that EV-loaded hydrogel treatment led to substantially greater alveolar bone height and better bone volume/tissue volume ratio, compared with treatment involving hydrogel alone (Fig. 3D). Immunofluorescence staining revealed that the expression level of Th17-related ROR γ was greater in the periodontitis group; this expression was inhibited by the injection of EV-loaded hydrogel ($P < 0.05$, Fig. 3E). Consistent with these findings, suppression of the Treg-related FOXP3 level in inflamed periodontal tissue was enhanced after EV-loaded hydrogel treatment ($P < 0.001$, Fig. 3E). These results suggested that hBMSC-derived EVs promoted the recovery of alveolar bone in an *in vivo* model of periodontitis.

miR-1246 from hBMSC-derived EVs regulated Th17/Treg homeostasis

After confirming the importance of hBMSC-derived EVs for T-cell differentiation in periodontitis, we further analyzed which miRNAs have central roles in such responses. EV-miRNA profiles with or without stimulation by *P. g.* LPS were examined by miRNA-seq. In total, 48 significantly upregulated and 101 significantly downregulated miRNAs were identified in the *P. g.* LPS-stimulated group. Heatmap, volcano plot, and principal component analysis assessments demonstrated the reduction of miR-1246 expression (Fig. 4A–C, Appendix Table 4). The grouping of miR-1246 transfection is shown in Fig. 4D, and the transfection efficiency test confirmed that the transfection was successful (Fig. 4E). Furthermore, naïve PD-CD4⁺ T cells were treated with EVs from hBMSCs or miR-1246 mimic/inhibitor-transfected hBMSCs. Flow cytometry assays revealed that the presence of miR-1246 in hBMSC-derived EVs contributed to the regulation of Th17/Treg homeostasis (Fig. 4F, G).

hBMSC-derived EV miR-1246 targeted ACE2 on CD4⁺ T cells and regulated the YAP1 signaling pathway

To investigate the function of EV-miR-1246, potential miR-1246 target genes were sought via miRDB, miRWalk, and TargetScan. In total, 216 intersections were identified in a Venn diagram (Fig. 5A, Appendix Table 5). *ACE2* is an important gene in periodontitis and CD4⁺ T-cell differentiation; miR-1246 could bind to the *ACE2* 3'-UTR (Fig. 5B). Dual-luciferase reporter assays confirmed that the activity of the *ACE2* 3'-UTR decreased upon transfection with hsa-miR-1246 ($P < 0.01$), suggesting that hsa-miR-1246 acts on the wild-type *ACE2* 3'-UTR (but not its mutant counterpart) (Fig. 5C). The expression of *ACE2* in CD4⁺ T cells was reduced by EVs overexpressing miR-1246, whereas the expression was increased by EVs containing miR-1246 inhibitor (Fig. 5F, G). We explored the *ACE2* interaction network using the STRING database (Fig. 5D). Furthermore, we found the top 5 most important pathways according to Kyoto

Encyclopedia of Genes and Genomes (KEGG) analysis, based on examination of miRNA-seq datasets (Fig. 5E, Appendix Table 6). Because there was strong support for the Hippo signaling pathway as a potential downstream pathway of hBMSC-derived EV-miRNAs, we analyzed this pathway. Our western blotting analysis showed that YAP1 expression was inhibited, whereas p-YAP1 (S127) was activated. Thus, we speculate that the YAP1/Hippo signaling pathway is regulated by EV-miR-1246 (Fig. 5F, G).

Discussion

The present study sheds light on the potential use of EVs derived from hBMSCs as a therapeutic strategy for periodontitis. Our data demonstrate that the Th17/Treg ratio was elevated in the peripheral blood of patients with periodontitis, and hBMSC-derived EVs have the ability to decrease this ratio in CD4⁺ T cells from periodontitis patients *in vitro*. Moreover, *in vivo* experiments showed that hBMSC-derived EVs could ameliorate experimental periodontitis in mice. Our study further identified EV-miR-1246 as a crucial factor in regulating the Th17/Treg ratio, as it significantly down-regulated this ratio *in vitro*. Mechanistically, this was accomplished through the suppression of ACE2 expression and increased p-Yes-associated protein (YAP)1/YAP1 ratio in CD4⁺ T cells.

In line with previous studies, an imbalance involving Th17 and Treg cells in periodontal tissue and an elevated Th17/Treg ratio in peripheral blood are both closely associated with the progression of periodontal inflammation and alveolar bone destruction [9,29,30]. Our study revealed that the Th17/Treg ratio was substantially elevated in periodontitis patients and LIP mice, compared with healthy volunteers or healthy mice. Thus, modulation of the Th17/Treg ratio may serve as a new approach to periodontitis treatment. This study showed that hBMSC-derived EVs can effectively reduce the Th17/Treg ratio in periodontitis, both *in vitro* and *in vivo*. Considering the present findings, the putative roles of hBMSC-derived EVs in Th17/Treg cell differentiation are summarized in Fig. 6.

In recent years, MSCs have emerged as a promising therapy for periodontal regeneration [31]. hBMSC-derived EVs suppressed macrophage inflammatory responses during exposure to *P. gingivalis* and promoted periodontal regeneration [13,17]. Consistently, our *in vivo* study demonstrated that hBMSC-derived EVs promoted periodontal regeneration in a mouse model. In our *in vitro* study, hBMSC-derived EVs restored Th17/Treg homeostasis, decreasing the Th17 cell population by 75%. Notably, in contrast to the periodontal ligament stem cell-derived EVs in the work of Zheng et al. [32], our hBMSC-derived EVs demonstrated more potent inhibition of Th17 differentiation.

In our *in vivo* study, LIP mice were injected with EV-loaded hydrogels. The hydrogel (F127) used in this study is reportedly safe and effective in periodontal repair applications [33]. We observed a similar therapeutic effect when the hydrogel was used alone. Furthermore, a significant synergistic effect was observed when LIP mice were treated with EV-loaded hydrogels. The decreased level of Th17-related ROR γ expression and increased level of Treg-related FOXP3 expression indicated that periodontal homeostasis had been restored, with the improvement of alveolar bone height.

P. gingivalis-associated miRNAs influence the innate immune response, whereas *P. g.* LPS may affect the nature of host miRNAs and their mRNA targets [34]. In the present study, stimulation with *P. g.* LPS led to the upregulation of 48 miRNAs and downregulation of 101 miRNAs in hBMSC-derived EVs. miRNA-seq revealed downregulation of miR-1246, which reportedly regulates Th17/Treg homeostasis in Henoch-Schönlein purpura [35] and hepatic ischemia/reperfusion injury [36]. Thus, we investigated the role of miR-1246 in the differentiation of CD4⁺ T cells in periodontitis. We sequenced EV-miRNAs from hBMSCs stimulated with or without *P. g.* LPS because the periodontitis microenvironment usually involves *P. g.* LPS. Our transfection analysis confirmed that miR-1246-overexpressing EVs could promote restoration of Th17/Treg homeostasis; this effect was reversed by the use of miR-1246 inhibitors. Zhang et al. sequenced EV-miRNAs derived from dental pulp stem cells cultured in two-dimensional and three-dimensional systems, and found that miR-1246 exhibited one of the most differential expression patterns [22]. Additionally, EV-miR-1246 derived from the stem cells of human deciduous exfoliated teeth reportedly inhibits angiogenesis and oral squamous cell carcinoma [37]. *In vivo*, antagomir-1246 reverses the effects of EVs in alveolar bone loss in mice with periodontitis [38]. Our findings extend the knowledge regarding miR-1246-specific regulatory effects in periodontal immunity, whereby hBMSC-derived EVs modified with an innovative miR-1246-mimic can exert an enhanced immunomodulatory effect on Th17/Treg homeostasis *in vitro*.

Through bioinformatics analysis and dual luciferase assays, we identified *ACE2* as the target gene of hBMSC-derived EV-miR-1246. A recent study showed that *ACE2* was the target gene of miR-146a and miR-155 in salivary glands and masticatory mucosa [24]. EVs containing miR-1246 inhibitor reduced *ACE2* expression in *Escherichia coli* LPS (*E. c.* LPS)-stimulated pulmonary endothelial cells [39]. In the present study, miR-1246-overexpressing EVs significantly inhibited *ACE2* expression in PD-CD4⁺ T cells. This disparity may be related to differences between *E. c.* LPS and *P. g.* LPS, as well as differences between pulmonary endothelial cells and PD-CD4⁺ T cells. Consistent with our findings, the inhibition of miR-1246 led to increased *ACE2* expression in the small airway epithelium of smokers [40]. In addition to *ACE2*, EV-miR-1246 has various target genes, such as nuclear factor of activated T cells 5 (NFAT5) in MSCs from inflamed periodontium [22] and glycogen synthase kinase 3 beta in human umbilical cord blood MSCs from hepatic tissues damaged by ischemia/reperfusion [36]. Further studies are needed to identify other possible targets of EV-miR-1246.

We found that hBMSC-derived EVs downregulated YAP1 expression, and this suppression was enhanced by exosomes overexpressing miR-1246, whereas the opposite trend was observed for p-YAP1. YAP1 (the unphosphorylated form) is located in the nucleus when the Hippo pathway is inactive. Activation of the Hippo pathway leads to the phosphorylation of YAP1; p-YAP1(S127) is located in the cytoplasm, where it mediates multiple downstream genes [41]. Our results suggested that lower expression of total YAP1 is associated with a lower Th17/Treg ratio, consistent with the findings by Zhou et al. [42] that abundant expression of YAP1 led to increased Th17 cell differentiation in patients with asthma exacerbation.

Declarations

Acknowledgments

The authors received the following financial support for the research, authorship, and/or publication of this article. This study was supported by the National Natural Science Foundation of China (82001008, 81901013), Science and Technology Commission of Shanghai Municipality (Pujiang Program, 20PJ1414400), Chinese Stomatological Association (Young Talent Project of Orthodontics, COS-B2021-05), and Shanghai Municipal Health Commission (Rising Star Young Physician Talent Project, 20RS88; Youth Scientific Research Project, 20204Y0097). We thank Figdraw for providing painting materials for Fig. 6. We also thank Ryan Chastain-Gross, Ph.D., from Liwen Bianji (Edanz) for editing the English text of a draft of this manuscript.

Competing Interests

The authors have declared that no competing interest exists.

Funding

The authors received the following financial support for the research, authorship, and/or publication of this article. This study was supported by the National Natural Science Foundation of China (82001008, 81901013), Science and Technology Commission of Shanghai Municipality (Pujiang Program, 20PJ1414400), Chinese Stomatological Association (Young Talent Project of Orthodontics, COS-B2021-05), and Shanghai Municipal Health Commission (Rising Star Young Physician Talent Project, 20RS88; Youth Scientific Research Project, 20204Y0097).

References

1. Kassebaum NJ, Smith AGC, Bernabé E, et al. Global, Regional, and National Prevalence, Incidence, and Disability-Adjusted Life Years for Oral Conditions for 195 Countries, 1990-2015: A Systematic Analysis for the Global Burden of Diseases, Injuries, and Risk Factors. *J Dent Res.* 2017;96(4):380-387.
2. Hajishengallis G, Chavakis T. Local and systemic mechanisms linking periodontal disease and inflammatory comorbidities. *Nat Rev Immunol.* 2021;21(7):426-440.
3. Yu B, Wang CY. Osteoporosis and periodontal diseases - An update on their association and mechanistic links. *Periodontol 2000.* 2022;89(1):99-113.
4. Gaffen SL, Moutsopoulos NM. Regulation of host-microbe interactions at oral mucosal barriers by type 17 immunity. *Sci Immunol.* 2020;5(43):eaau4594.

5. Pan W, Wang Q, Chen Q. The cytokine network involved in the host immune response to periodontitis. *Int J Oral Sci.* 2019;11(3):30.
6. Liao C, Zhang C, Yang Y. Pivotal Roles of Interleukin-17 as the Epicenter of Bone Loss Diseases. *Curr Pharm Des.* 2017;23(41):6302-6309.
7. Liao C, Cheng T, Wang S, Zhang C, Jin L, Yang Y. Shear stress inhibits IL-17A-mediated induction of osteoclastogenesis via osteocyte pathways. *Bone.* 2017;101:10-20.
8. Liao C, Zhang C, Jin L, Yang Y. IL-17 alters the mesenchymal stem cell niche towards osteogenesis in cooperation with osteocytes. *J Cell Physiol.* 2020;235(5):4466-4480.
9. Deng J, Lu C, Zhao Q, Chen K, Ma S, Li Z. The Th17/Treg cell balance: crosstalk among the immune system, bone and microbes in periodontitis. *J Periodontal Res.* 2022;57(2):246-255.
10. Cafferata EA, Castro-Saavedra S, Fuentes-Barros G, et al. Boldine inhibits the alveolar bone resorption during ligature-induced periodontitis by modulating the Th17/Treg imbalance. *J Periodontol.* 2021;92(1):123-136.
11. Hajishengallis G. Interconnection of periodontal disease and comorbidities: Evidence, mechanisms, and implications. *Periodontol 2000.* 2022;89(1):9-18.
12. Martin I, Galipeau J, Kessler C, Le Blanc K, Dazzi F. Challenges for mesenchymal stromal cell therapies. *Sci Transl Med.* 2019;11(480):eaat2189.
13. Yue C, Cao J, Wong A, et al. Human Bone Marrow Stromal Cell Exosomes Ameliorate Periodontitis. *J Dent Res.* 2022;101(9):1110-1118.
14. Xu XY, Li X, Wang J, He XT, Sun HH, Chen FM. Concise Review: Periodontal Tissue Regeneration Using Stem Cells: Strategies and Translational Considerations. *Stem Cells Transl Med.* 2019;8(4):392-403.
15. Spees JL, Lee RH, Gregory CA. Mechanisms of mesenchymal stem/stromal cell function. *Stem Cell Res Ther.* 2016;7(1):125. Published 2016 Aug 31.
16. Lei F, Li M, Lin T, Zhou H, Wang F, Su X. Treatment of inflammatory bone loss in periodontitis by stem cell-derived exosomes. *Acta Biomater.* 2022;141:333-343.
17. Liu L, Guo S, Shi W, et al. Bone Marrow Mesenchymal Stem Cell-Derived Small Extracellular Vesicles Promote Periodontal Regeneration. *Tissue Eng Part A.* 2021;27(13-14):962-976.
18. Gebert LFR, MacRae IJ. Regulation of microRNA function in animals. *Nat Rev Mol Cell Biol.* 2019;20(1):21-37.
19. Naqvi AR, Slots J. Human and herpesvirus microRNAs in periodontal disease. *Periodontol 2000.* 2021;87(1):325-339.

20. Luan X, Zhou X, Naqvi A, et al. MicroRNAs and immunity in periodontal health and disease. *Int J Oral Sci.* 2018;10(3):24. Published 2018 Aug 6.
21. Naqvi RA, Datta M, Khan SH, Naqvi AR. Regulatory roles of MicroRNA in shaping T cell function, differentiation and polarization. *Semin Cell Dev Biol.* 2022;124:34-47.
22. Zhang Y, Chen J, Fu H, et al. Exosomes derived from 3D-cultured MSCs improve therapeutic effects in periodontitis and experimental colitis and restore the Th17 cell/Treg balance in inflamed periodontium. *Int J Oral Sci.* 2021;13(1):43. Published 2021 Dec 14.
23. Welch JL, Xiang J, Chang Q, Houtman JCD, Stapleton JT. T-Cell Expression of Angiotensin-Converting Enzyme 2 and Binding of Severe Acute Respiratory Coronavirus 2. *J Infect Dis.* 2022;225(5):810-819.
24. Roganović JR. microRNA-146a and -155, upregulated by periodontitis and type 2 diabetes in oral fluids, are predicted to regulate SARS-CoV-2 oral receptor genes. *J Periodontol.* 2021;92(7):35-43.
25. Meng KP, Majedi FS, Thauland TJ, Butte MJ. Mechanosensing through YAP controls T cell activation and metabolism. *J Exp Med.* 2020;217(8):e20200053.
26. Stampouloglou E, Cheng N, Federico A, et al. Yap suppresses T-cell function and infiltration in the tumor microenvironment. *PLoS Biol.* 2020;18(1):e3000591. Published 2020 Jan 13.
27. Tonetti MS, Greenwell H, Kornman KS. Staging and grading of periodontitis: Framework and proposal of a new classification and case definition [published correction appears in *J Periodontol.* 2018 Dec;89(12):1475]. *J Periodontol.* 2018;89 Suppl 1:S159-S172.
28. Lin L, Li S, Hu S, et al. UCHL1 Impairs Periodontal Ligament Stem Cell Osteogenesis in Periodontitis. *J Dent Res.* 2023;102(1):61-71.
29. Tsukasaki M, Komatsu N, Nagashima K, et al. Host defense against oral microbiota by bone-damaging T cells. *Nat Commun.* 2018;9(1):701. Published 2018 Feb 16.
30. Su X, Zhang J, Qin X. CD40 up-regulation on dendritic cells correlates with Th17/Treg imbalance in chronic periodontitis in young population. *Innate Immun.* 2020;26(6):482-489.
31. Chen FM, Gao LN, Tian BM, et al. Correction to: Treatment of periodontal intrabony defects using autologous periodontal ligament stem cells: a randomized clinical trial. *Stem Cell Res Ther.* 2018;9(1):260. Published 2018 Oct 7.
32. Zheng Y, Dong C, Yang J, et al. Exosomal microRNA-155-5p from PDLSCs regulated Th17/Treg balance by targeting sirtuin-1 in chronic periodontitis. *J Cell Physiol.* 2019;234(11):20662-20674.
33. Almoshari Y, Ren R, Zhang H, et al. GSK3 inhibitor-loaded osteotropic Pluronic hydrogel effectively mitigates periodontal tissue damage associated with experimental periodontitis. *Biomaterials.*

2020;261:120293.

34. Lv PY, Gao PF, Tian GJ, et al. Osteocyte-derived exosomes induced by mechanical strain promote human periodontal ligament stem cell proliferation and osteogenic differentiation via the miR-181b-5p/PTEN/AKT signaling pathway. *Stem Cell Res Ther.* 2020;11(1):295. Published 2020 Jul 17.
35. Li J, Chen M, Wang J, Lu L, Li X, Le Y. MicroRNA profiling in Chinese children with Henoch-Schonlein purpura and association between selected microRNAs and inflammatory biomarkers. *Acta Paediatr.* 2021;110(7):2221-2229.
36. Xie K, Liu L, Chen J, Liu F. Exosomes derived from human umbilical cord blood mesenchymal stem cells improve hepatic ischemia reperfusion injury via delivering miR-1246. *Cell Cycle.* 2019;18(24):3491-3501.
37. Liu P, Zhang Q, Mi J, et al. Exosomes derived from stem cells of human deciduous exfoliated teeth inhibit angiogenesis in vivo and in vitro via the transfer of miR-100-5p and miR-1246. *Stem Cell Res Ther.* 2022;13(1):89.
38. Shen Z, Kuang S, Zhang Y, et al. Chitosan hydrogel incorporated with dental pulp stem cell-derived exosomes alleviates periodontitis in mice via a macrophage-dependent mechanism. *Bioact Mater.* 2020;5(4):1113-1126.
39. Fang Y, Gao F, Hao J, Liu Z. microRNA-1246 mediates lipopolysaccharide-induced pulmonary endothelial cell apoptosis and acute lung injury by targeting angiotensin-converting enzyme 2. *Am J Transl Res.* 2017;9(3):1287-1296.
40. Zhang H, Rostami MR, Leopold PL, et al. Expression of the SARS-CoV-2 ACE2 Receptor in the Human Airway Epithelium. *Am J Respir Crit Care Med.* 2020;202(2):219-229.
41. Meng Z, Moroishi T, Guan KL. Mechanisms of Hippo pathway regulation. *Genes Dev.* 2016;30(1):1-17.
42. Zhou J, Zhang N, Zhang W, Lu C, Xu F. The YAP/HIF-1 α /miR-182/EGR2 axis is implicated in asthma severity through the control of Th17 cell differentiation. *Cell Biosci.* 2021;11(1):84. Published 2021 May 12.

Figures

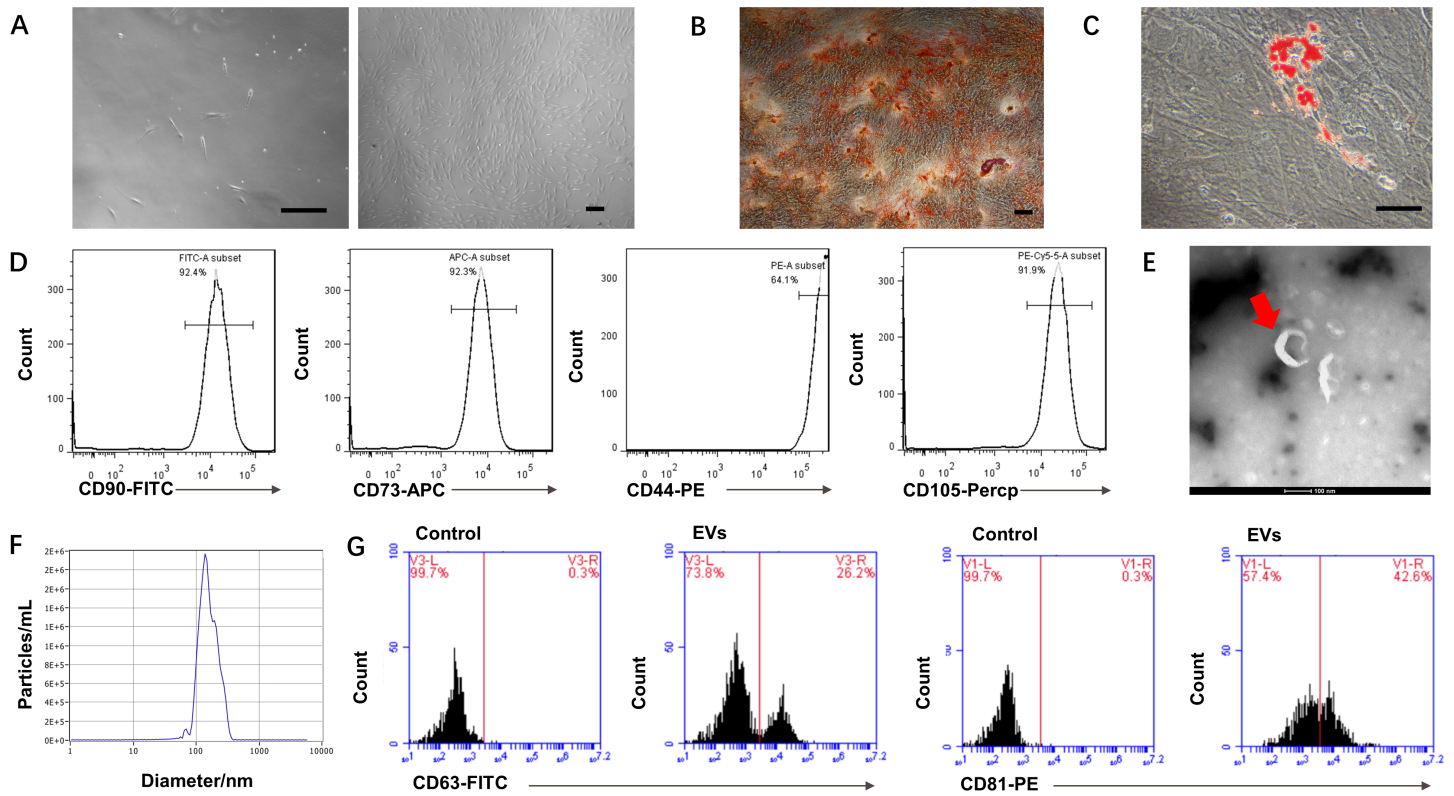


Figure 1

Extraction and identification of hBMSCs and hBMSC-derived EVs. **(A)** Cell morphology of hBMSCs from periodontally healthy volunteers (bar = 100 μ m). **(B)** Alizarin red S staining of calcium deposits in hBMSCs (bar = 100 μ m). **(C)** Oil red O staining of oil droplets in hBMSCs (bar = 100 μ m). **(D)** The hBMSC-specific markers CD90 (92.4%), CD44 (64.1%), CD105 (91.9%), and CD73 (92.3%) were detected by flow cytometry. **(E)** Transmission electron micrographs of hBMSC-derived EVs. **(F)** Particle sizes of hBMSC-derived EVs, as determined by nanoparticle tracking analysis (NTA). **(G)** Positive expression of CD63 and CD81 in isolated EVs, as determined by flow cytometry.

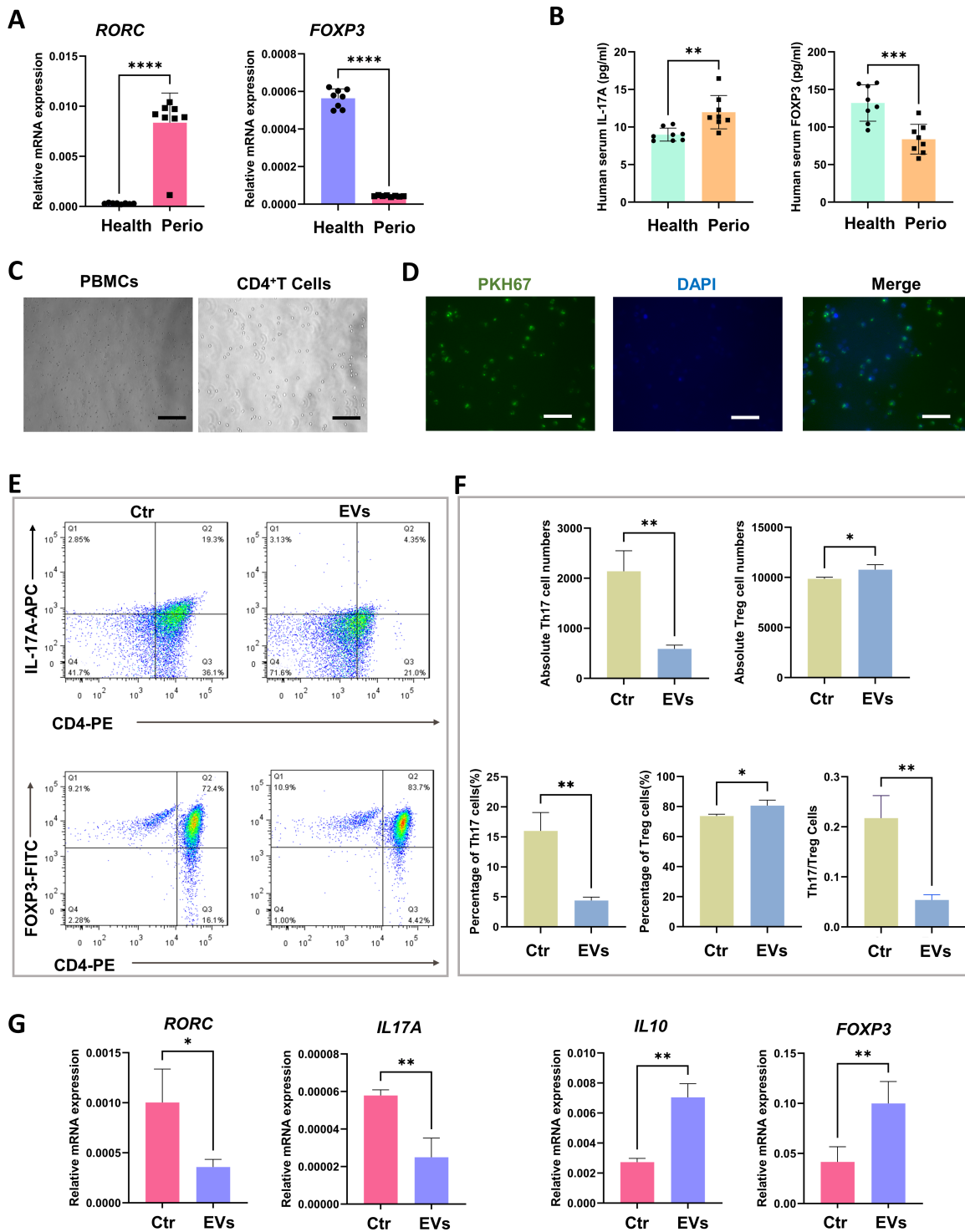


Figure 2

hBMSC-derived EVs reduced the Th17/Treg ratio in CD4⁺ T cells from periodontitis patients. (A) The mRNA expression level of *RORC* was upregulated and the mRNA expression level of *FOXP3* was downregulated in CD4⁺ T cells from peripheral blood of periodontitis patients, compared with healthy controls. (B) The level of IL-17A was upregulated and the level of FOXP3 was downregulated in peripheral blood from periodontitis patients, compared with healthy controls detected by ELISA. (C) Micrographs of

PBMCs and purified naïve CD4⁺ T cells from periodontitis patients (bar = 100 μm). (D) PKH67-stained hBMSC-derived EVs (green) and 4',6-diamidino-2-phenylindole (DAPI)-stained CD4⁺ T cells (nuclei, blue) (bar = 100 μm). (E) Flow cytometry analysis of Th17 and Treg cells after the uptake of hBMSC-derived EVs. (F) Absolute counts and percentages of Th17 and Treg cells showed that hBMSC-derived EVs decreased the Th17/Treg ratio. (G) mRNA expression levels of *RORC*, *IL17A*, *IL10*, and *FOXP3* genes in CD4⁺ T cells after stimulation with EVs. **P* < 0.05; ***P* < 0.01; ****P* < 0.001.

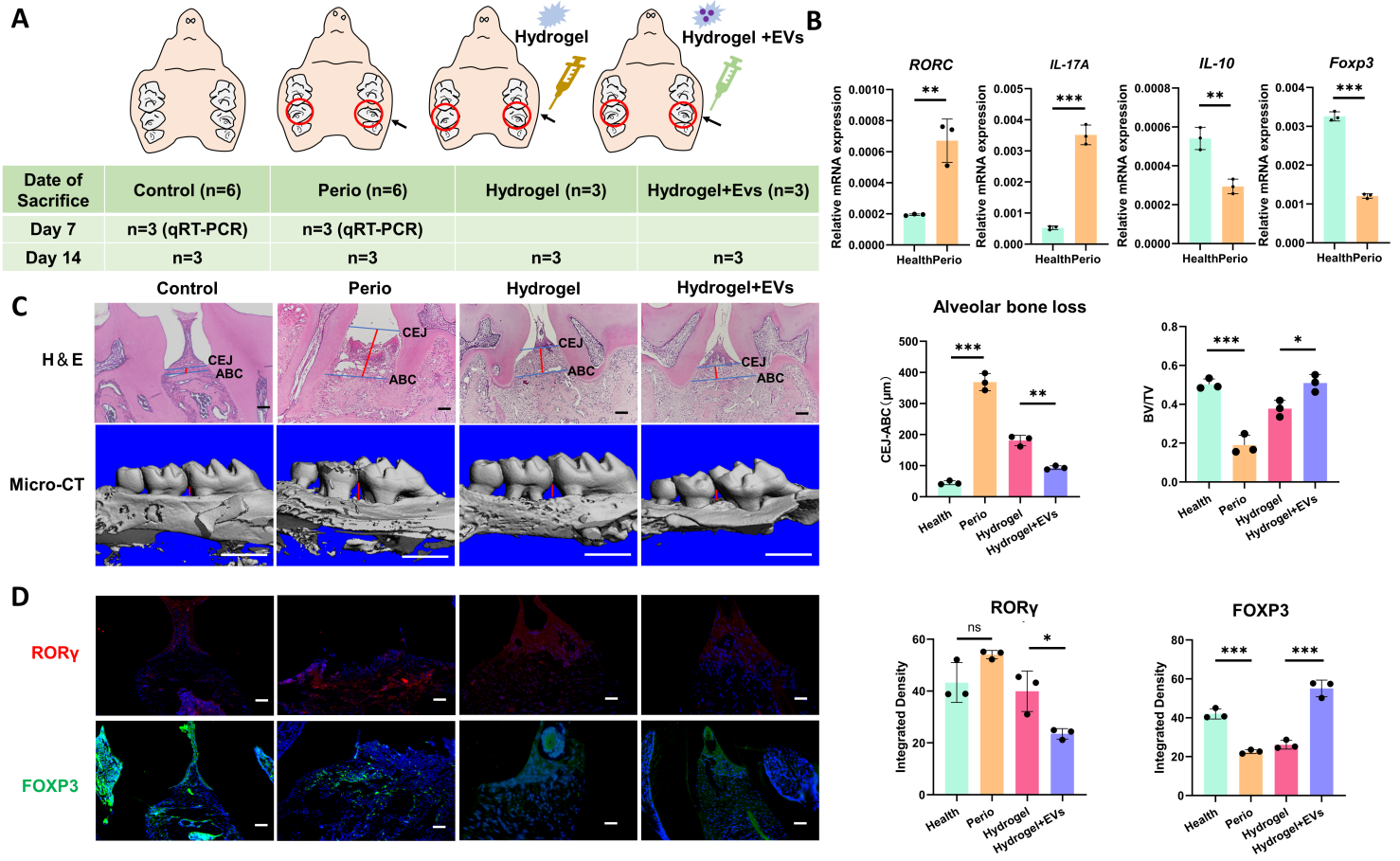


Figure 3

hBMSC-derived EVs reduced the Th17/Treg ratio and alleviated alveolar bone loss *in vivo*. (A) Modeling schematic diagram. (B) mRNA expression levels of *Rorc*, *Il17a*, *Il10*, and *Foxp3* in gingival tissue from mice with or without periodontitis. (C) Histological staining and micro-CT: blue lines represent distance between alveolar bone crest (ABC) and cemento-enamel junction (CEJ), whereas red lines represent bone loss (bar = 100 μm). Quantitative analysis of alveolar bone height loss via hematoxylin and eosin (H&E) staining, and quantitative analysis of bone absorption density via micro-CT. (D) Immunofluorescence labeling and quantitative analysis of RORγ (red) and FOXP3 (green) (bar = 100 μm); negative controls are shown in Appendix Fig. 2. **P* < 0.05; ***P* < 0.01; ****P* < 0.001

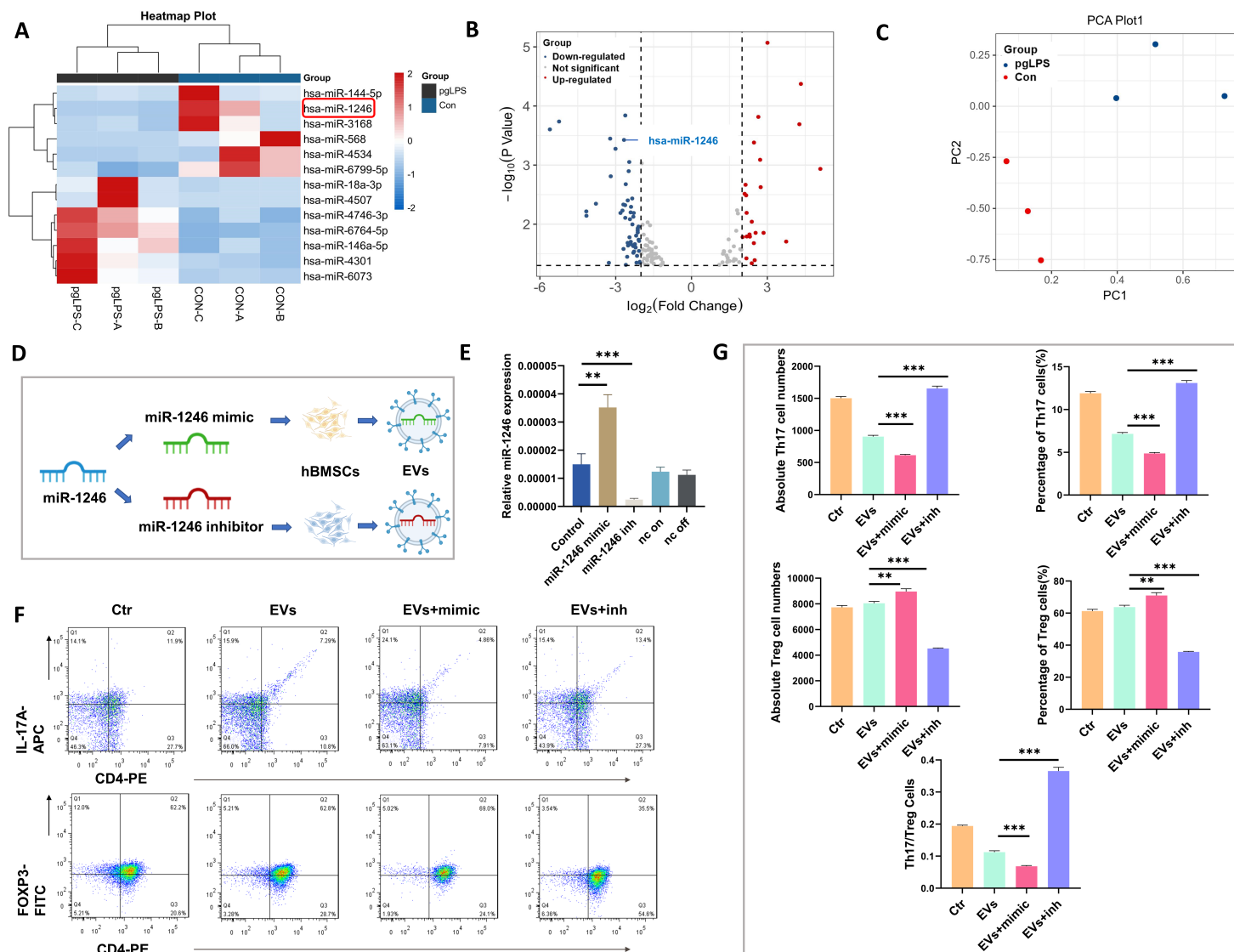


Figure 4

hBMSC-derived EV-miR-1246 reduced the Th17/Treg ratio. **(A)** Heatmap of EV-miRNA levels from hBMSCs stimulated with or without *P. g.* LPS ($n = 3$ per group). **(B)** Volcano plots showing differences in EV-miRNA expression in hBMSCs stimulated with *P. g.* LPS versus PBS control. x-axis: \log_2 fold change, y-axis: $-\log_{10}$ (p-value). **(C)** Principal component analysis of EV-miRNAs from *P. g.* LPS group and control group. **(D)** Schematic diagram of transfection involving miR-1246 mimic and inhibitor. **(E)** Expression levels of miR-1246 in hBMSC-derived EVs after transfection (nc on vs. mimic, nc off vs. inhibitor). **(F)** Flow cytometry analysis of Th17 (CD4⁺ IL-17A⁺) and Treg (CD4⁺ FOXP3⁺) cells among CD4⁺ T cells stimulated with transfected EVs. **(G)** Statistical analysis of Flow cytometry (Th17/Treg cell numbers, percentages, and ratios). The reduction in Th17/Treg ratio after treatment with normal EVs was further suppressed by transfection with miR-1246 mimic, which was reversed by EVs containing miR-1246 inhibitor. * $P < 0.05$; ** $P < 0.01$; *** $P < 0.001$

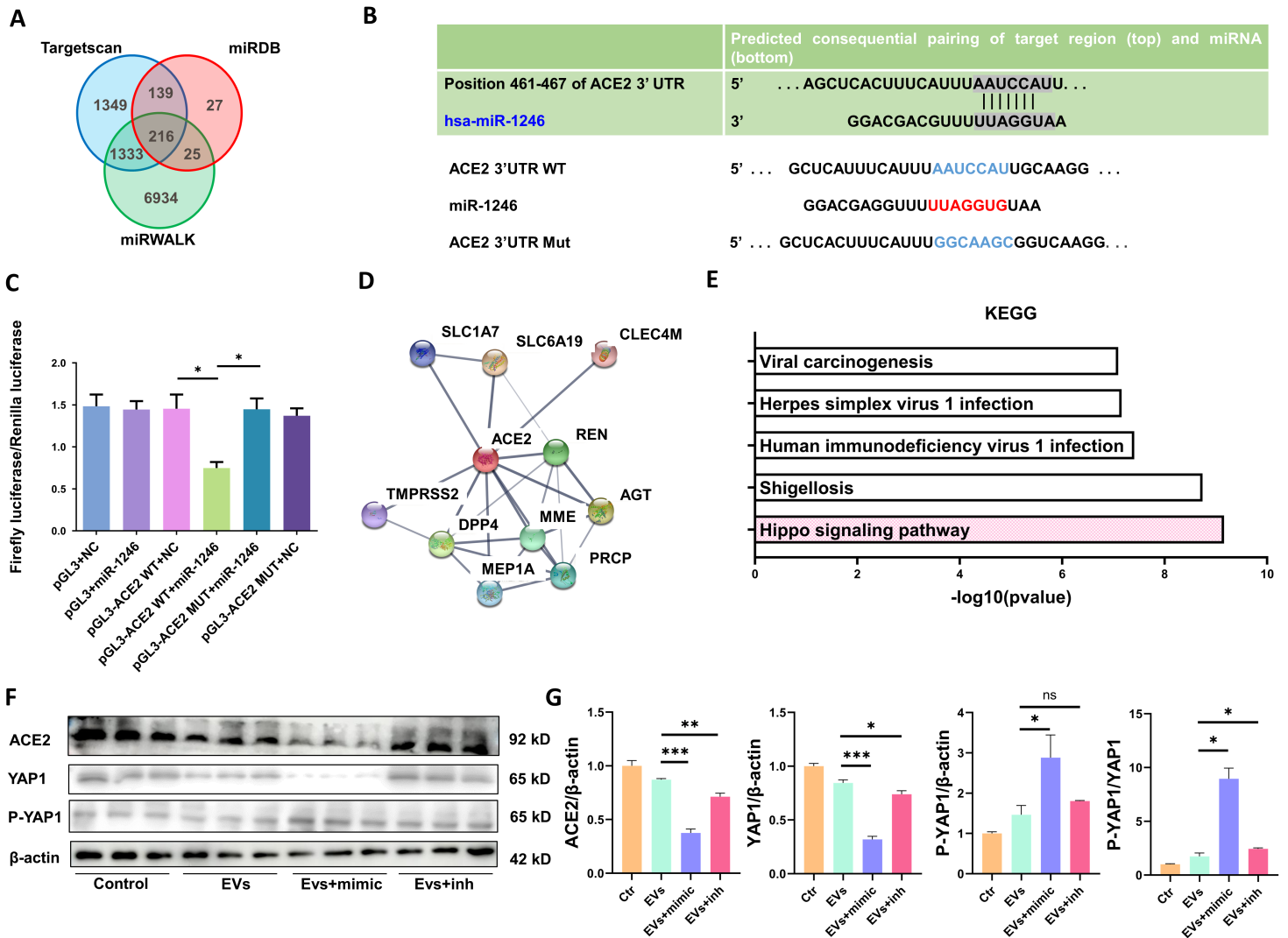


Figure 5

EV-miR-1246 targeted *ACE2* and regulated the Hippo signaling pathway in CD4⁺ T cells. **(A)** Venn diagram showing the intersection of 216 potential miR-1246 target genes. **(B)** Predicted active sites of miR-1246 and *ACE2*. Binding sites in the *ACE2* 3'-UTR were targeted by miR-1246. **(C)** Luciferase reporter assays confirmed that miR-1246 regulated the 3'UTR of the target gene *ACE2*. **(D)** STRING diagram showing proteins associated with *ACE2*. **(E)** Kyoto Encyclopedia of Genes and Genomes (KEGG) functional analysis revealed miRNAs that were strongly associated with several pathways, including the Hippo signaling pathway. **(F, G)** Western blotting analysis showed that the p-YAP1 (S127)/YAP1 ratio in CD4⁺ T cells was increased by hBMSC-derived EVs and further increased in the presence of EVs overexpressing miR-1246, whereas it was decreased in the miR-1246 inhibitor group. *ACE2* exhibited opposite effects in the presence of miR-1246 or miR-1246 inhibitor. * $P < 0.05$; ** $P < 0.01$; *** $P < 0.001$

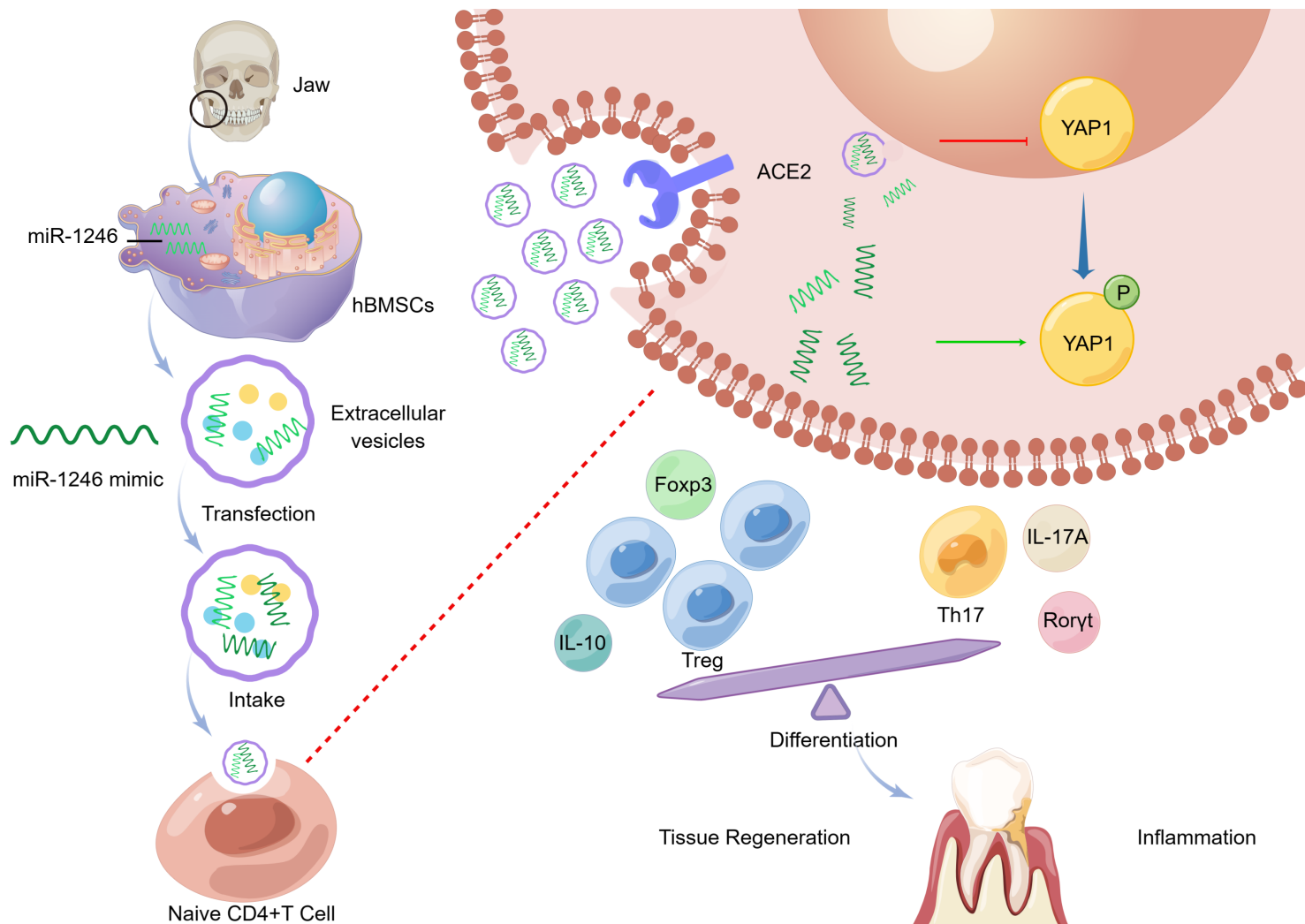


Figure 6

Schematic showing roles of hBMSC-derived EVs in Th17/Treg cell differentiation. hBMSC-derived EVs modulate Th17/Treg homeostasis by transferring miR-1246, which targets ACE2 and regulates the YAP1/Hippo signaling pathway in naïve PD-CD4⁺ T cells. Elevated expression of EV-miR-1246 inhibits periodontal inflammation and promotes tissue regeneration.

Supplementary Files

This is a list of supplementary files associated with this preprint. Click to download.

- [20230328supplementary.docx](#)